

Supporting Information

Boosting Alkaline Hydrogen Evolution through Cobalt-Regulated *d*-Band Center of Metallic Molybdenum and Concurrent Nitrogen-Doping

Bo Geng^{a*}, Qingyang Song^a, Rui Chen^a, and Gaojie Li^a

^a School of Physics and Engineering, Henan University of Science and Technology,
Luoyang 471023, China.

*Corresponding authors.

E-mail addresses: gengbo_wl@163.com.

1. Chemicals

All the chemicals were directly used as received without further purification. All the chemicals were directly used as received without further purification. Melamine was purchased from Tianjin Guangfu Fine Chemical Research Institute (China). Ammonium paramolybdate was purchased from Tianjin Komeo Chemical Reagent Co., Ltd. Cobalt acetate tetrahydrate was purchased from China Pharmaceutical Group Chemical Reagents Co., Ltd. Anhydrous N,N-dimethylformamide was purchased from Xilong Science Co., Ltd. Pt/C (20% Pt on Vulcan XC-72R) was purchased from Sigma-Aldrich Chemical Reagent Co., Ltd. Carbon cloth and Nafion solution (5.0 wt%) were purchased from Kunshan Yiersheng International Trade Co. Ltd (Kunshan, China). Graphite rod and Ag/AgCl (KCl saturated) electrode were purchased from AIDA Science-Technology Development Co., Ltd (Tianjin, China). All aqueous solutions were prepared using ultrapure water ($>18\text{ M}\Omega$).

2. Physical characterizations

The crystallographic structure of the synthesized samples was analyzed by X-ray diffraction (XRD) using a Bruker D8 ADVANCE diffractometer equipped with a monochromatic Mo K α radiation source ($\lambda = 0.15406\text{ nm}$). Phase identification was conducted over a 2θ range of $10\text{--}80^\circ$ with a step size of 0.02° . Surface chemical states and elemental composition were examined by X-ray photoelectron spectroscopy (XPS) on a Thermo Scientific Escalab 250Xi system with an Al K α X-ray source (1486.6 eV). All binding energies were calibrated using the C 1s peak (284.8 eV) as an internal reference. Morphological and microstructural features were investigated using field-emission scanning electron microscopy (FE-SEM, Hitachi S-5200) and high-resolution transmission electron microscopy (HR-TEM, FEI Tecnai-F20) equipped with an energy-filtering system (Gatan Imaging Filter). Elemental distribution was further verified by energy-dispersive X-ray spectroscopy (EDS) mapping during TEM analysis. ICP mass spectrometry was carried out by using a Thermo iCAP 6000 ICP-MS.

3. The TOF calculation.

The turnover frequency (TOF) for each active site was determined employing methods previously reported. First, we performed cyclic voltammograms in phosphate buffer (pH = 7) with a scan rate of 50 mV s⁻¹ to examine the number of active sites (n). Then the number of the voltammetric charges (Q) could be obtained after deduction of the blank value. Therefore, n (mol) and TOF (s⁻¹) can be determined toward HER with the following equation:

$$n = Q / 2F$$

$$TOF = j * S_{geo} / 2 * F * n$$

where j is the measured current density, S_{geo} is the surface area of CFC, F is Faraday constant (96485.3 C mol⁻¹). Toward OER, the n (mol) and TOF (s⁻¹) can be determined with the following equation:

$$n = Q / 4F$$

$$TOF = j * S_{geo} / 4 * F * n$$

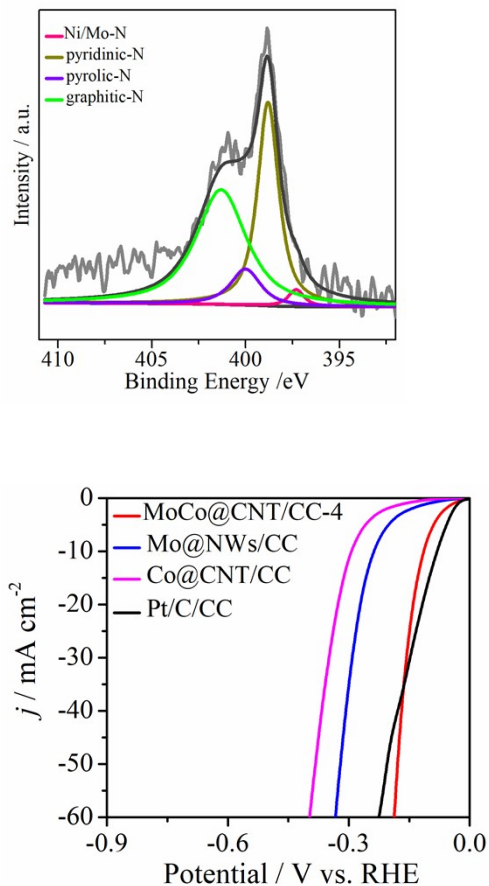
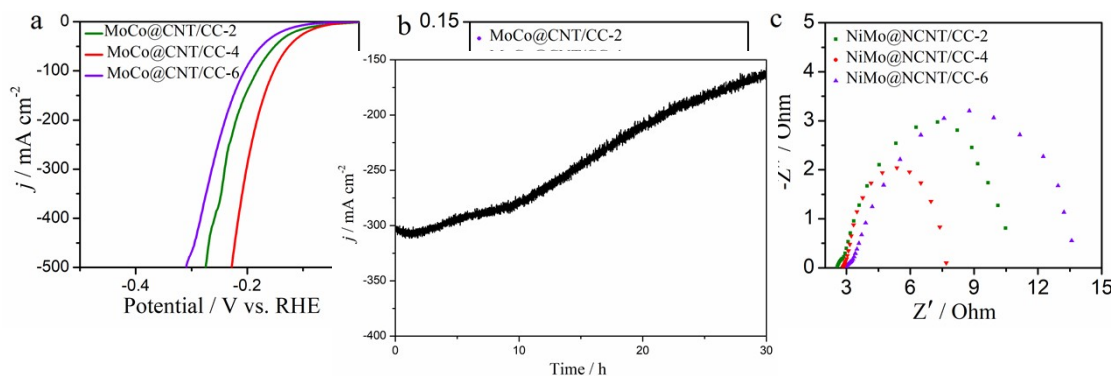


Figure S1 N 1s XPS spectra of MoCo@CNT/CC-4.

Figure S2. The mass loading-normalized polarization curves of Pt/C/CC, MoCo@NCNT/CC, Mo@NWs/CC and Co@NCNT/CC toward HER in alkaline media.

Figure S3 a) LSV curves, b) Tafel slopes, c) EIS spectra of MoCo@CNT/CC-2, MoCo@CNT/CC-4, and MoCo@CNT/CC-6 toward HER in alkaline media.

Figure S4 The time-dependent current density curve of Pt/C/CC in 1 M KOH.



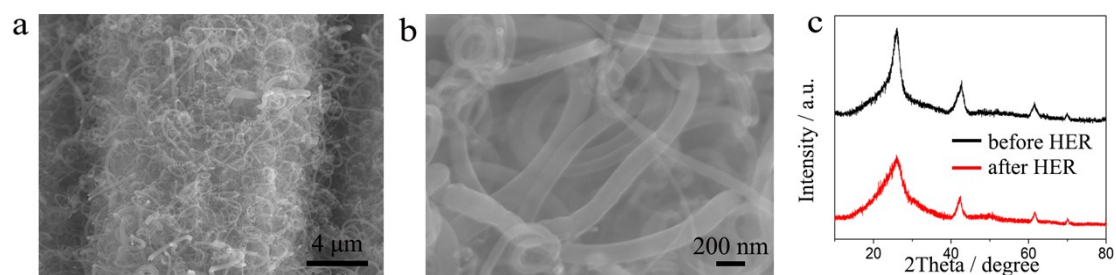


Figure S5 a-b) SEM images, c) XRD patterns of MoCo@CNT/CC-4 after stability tests for HER in 1 M KOH media

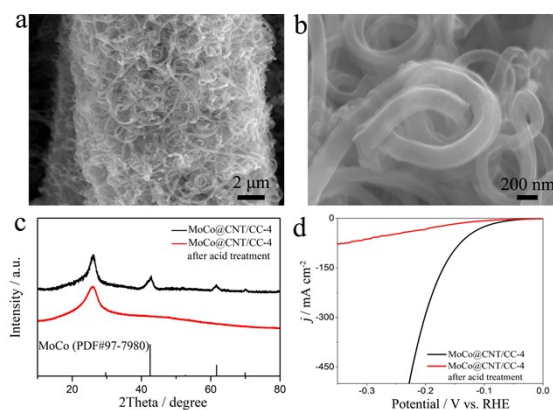


Figure S6 a-b) SEM images, c) XRD of MoCo@CNT/CC-4 after acid treatment, d) LSV curves of MoCo@CNT/CC-4 and MoCo@CNT/CC-4 after acid treatment toward HER in 1 M KOH media (acid treatment: 3.0 M HCl solution at room temperature for 15 h).

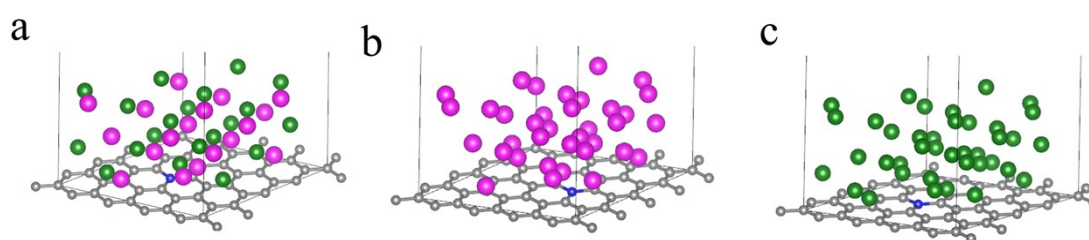


Figure S7 Schematic model of (a) MoCo@CNT-4, (b) Mo@NWs and (c) Co@CNT, respectively.

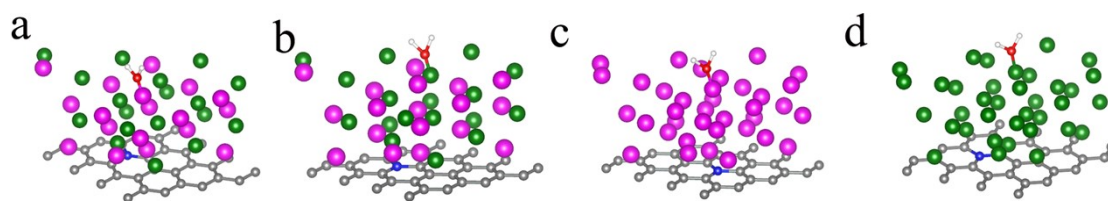


Figure S8 a-d) The side view optimized calculation models of Mo and Ni sites of MoCo@CNT-4, Mo@NWs/CC and Ni@CNT for adsorbed H₂O*.

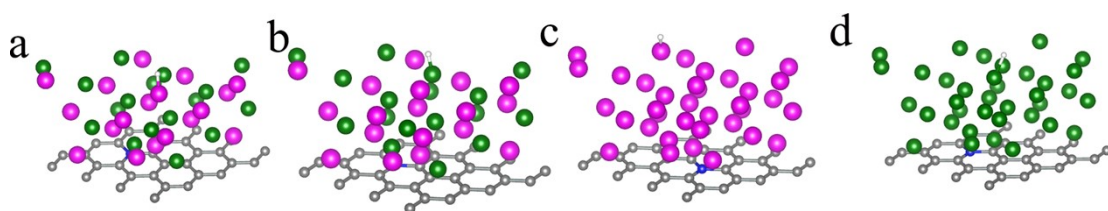


Figure S9 a-d) The side view optimized calculation models of Mo and Ni sites of MoCo@CNT-4, Mo@NWs/CC and Ni@CNT for adsorbed H*.

Table S1. Elemental composition of MoCo@CNT/CCs by ICP method.

sample	Mo (wt%)	Co (wt%)	atomic ratio (Mo/Co)
MoCo@CNT/CC-2	39.6	17.2	1.41
MoCo@CNT/CC-4	33.5	21.3	0.96
MoCo@CNT/CC-6	28.8	23.6	0.75

Table S2. Comparison of HER activities between our catalysts and those of recently reported electrocatalysts in 1 M KOH electrolyte.

Catalyst	η (mV) at 10 mA/cm ²	Tafel slope (mV/dec)	Reference
MoCo@CNT/CC-4	64	47.8	This work
MoCoCu	49	46	<i>Adv. Energy Mater.</i> , 2025, 2501852
Fe ₄ -NiS ₂ /MXene	148	85	<i>Appl. Catal. B-Environ. Energy</i> , 2025, 378, 125611
BP/CoNiSe ₂	82	64	<i>Appl. Catal. B-Environ. Energy</i> , 2025, 378, 125588
hcp Pt-Ni alloy	65	78	<i>Nat. Commun.</i> 2017, 8,

			15131
NiNi ₂ S ₄ /NF	106	92.1	<i>Adv. Funct. Mater.</i> , 2016, 26, 4661-4672
NiNi ₂ N/NF	151	79	<i>ChemSusChem</i> , 2017, 10: 4170-4177
Ni ₃ (VO ₄) ₂ @NiNi ₂ O ₄ /NF	113	101	<i>Electrochim. Acta</i> , 2017, 256: 100-109
NiFeZr oxides/NF	104	119.3	<i>Adv. Mater.</i> , 2019, 31, 1901439
NiSe/NF	111	121.2	<i>Small</i> , 2018, 21, 1800763
Mo ₁ Ni ₂ -N/CFC	71.4	106.5	<i>Adv. Energy Mater.</i> , 2019, 9, 1900390
NiO/NC/TF	105	125	<i>Adv. Energy Mater.</i> , 2019, 9, 1803970
MoCo pre@ZnO/NF	134	92	<i>Adv. Energy Mater.</i> , 2019, 9, 1902703
Cr-Ni(OH)F/CC	95	118	<i>Adv. Energy Mater.</i> , 2019, 9, 1902449
NiP ₂ -FeP ₂ /CFP	115	89	<i>ACS Energy Lett.</i> , 2021, 6, 354-363